

Development of a High Detection Efficiency and Low-Cost Imaging Gamma-Ray Camera γ I

M. Kagaya*

College of Science, Ibaraki University, Japan

E-mail: 13nd401n@vc.ibaraki.ac.jp

R. Enomoto^{b,g}, R. Hanafusa^c, Y. Itoh^c, H. Katagiri^{a,g}, H. Muraishi^{d,g}, K. Nakayama^{a,g}, K. Satoh^e, T. Takeda^d, M. M. Tanaka^{f,g}, T. Uchida^{f,g}, T. Watanabe^{d,g}, S. Yanagita^{a,g}, T. Yoshida^{a,g}

Ibaraki University^a, Institute for Cosmic Ray Research University of Tokyo^b, Fuji Electric Co.^c, Kitasato University^d, Shinsei Corporation^e, KEK^f, Open-It^g

We developed a novel Compton camera γ I using CsI (TI) scintillators which has high detection efficiency and is low-cost. Our motivation for the development of this detector is measuring gamma rays produced by radioactive nuclides from Fukushima Daiichi Nuclear Power Plant accident. Our detector consists of two arrays of detectors which act as a Compton scatterer and absorber. Energies deposited by Compton scattered electrons and subsequent photoelectric absorption measured by photomultipliers are used for image reconstruction. Each array consists of 8 large CsI (TI) scintillator cubes, 3.5 cm on a side, which are inexpensive and have good energy resolution. The angular resolution is around 3.5° by using an image sharpening technique, and the detection efficiency is typically more than 10 times better than other detectors for the same purpose. We did measurement tests for contaminated area around $1 \mu\text{Sv/h}$. The imaging capability was verified by test measurements in Fukushima Prefecture together with the laboratory tests. In this paper, we reported the development of γ I and the results of the measurement tests.

*Technology and Instrumentation in Particle Physics 2014,
2-6 June, 2014
Amsterdam, the Netherlands*

*Speaker.

1. Introduction

The great east Japan earthquake occurred in 2011. Fukushima Daiichi Nuclear Power Plant had a hydrogen explosion. A large amount of radio active nuclides was released to the atmosphere, and a large area of eastern Japan was contaminated. The radiation exposure of residents remains a serious problem in Japan. Decontamination operation is extremely important, and it is immediately required. When we do decontamination operation, we usually use survey meters to measure radiation dose rate to find hot spots. However, with this method, it takes a long time to get the distribution map of radiation dose rate even for a small area. For this reason, we need a detector to visualize gamma rays to find hot spots.

Pin hole cameras (e.g. [1]) and Compton cameras (e.g. [2]) can be used for gamma-ray imaging. In measurement for contamination area in Fukushima, we need high detection efficiency and a wide field of view. Moreover, cost is essential because many detectors are needed for covering a large contamination area. However, in the case of a pin-hole camera, the detection efficiency is limited by the geometrical area of a pinhole. Another type of imaging gamma-ray camera is a Compton camera. The detection efficiency of this camera is better than the pin-hole camera and it has a wide field of view. Therefore we adopt a Compton camera for visualization of distribution of gamma rays.

Some Compton cameras have already been developed for measuring distribution of gamma rays from Fukushima Daiichi Nuclear Power Plant accident. One is the Compton camera using semiconductor [3]. This type of camera has high angular resolution ($\Delta\theta = 3^\circ$) due to its good energy resolution ($\frac{\Delta E}{662\text{keV}} = 2.2\%$ (FWHM)). However, it cannot be a low-cost mass production because it costs a lot ($> \$300,000$) to manufacture with moderate detection efficiency. Another type of Compton camera uses two $5\text{ cm} \times 5\text{ cm} \times 1\text{ cm}$ Ce doped $\text{Gd}_3\text{Al}_2\text{Ga}_3\text{O}_{12}$ (Ce:GAGG) scintillators [4]. This Compton camera is compact. However, this detector is also expensive (about $\$100,000$). For this reason, to measure a large contamination area with the dose rate around $1\ \mu\text{Sv/h}$ is difficult by using these detectors. Therefore we developed a novel Compton camera by using many CsI (TI) large scintillators which are inexpensive and have high mass thickness.

2. Method

2.1 Compton camera

A Compton camera is a visualizing technology that specifies the arrival direction of gamma rays from radiation sources. This technology uses Compton scattering which is the dominant interaction process of gamma ray in the energy of 662 keV for ^{137}Cs . A Compton camera typically consists of one scatter detector and one absorber detector (Fig. 1). In the case of ideal, a gamma ray from radiation source is Compton scattered in a scatterer and then photo-absorbed in an absorber. The locations and energy deposition of both interactions are measured by each detector. Then Compton kinematics allows us to calculate the scattering angle of an incident gamma ray by using the following equation.

$$\cos \theta = 1 - m_e c^2 \left(\frac{1}{E_2} - \frac{1}{E_1 + E_2} \right), \quad (2.1)$$

where, E_1 denotes the energy of the recoil electron, E_2 is the energy of the scattered gamma-ray photon, θ is the scattering angle, m_e is the electron mass, and c is the speed of light. The probability distribution of location of a radiation source is estimated with a circle by back-projection. The position of a radiation source can be reconstructed by intersecting all the reconstructed circles.

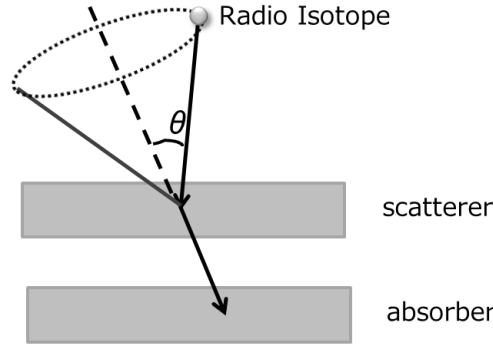


Figure 1: Conceptual design of Compton camera. It consists of scatterer and absorber.

2.2 Concept of our developed camera: γ I

The requirements of our detector are high detection efficiency and low-cost with moderate angular resolution. To achieve the requirements, a position sensitive detector which has high mass thickness at low-cost is needed. Thus we adopt scintillator detectors. In general, it seems that scintillator detectors are not suitable for a Compton camera due to lower energy resolution than semi-conductor detectors. However, if the incident energy of gamma rays (E_γ) is known, it is possible that the incident energy is given by the sum of E_1 and E_2 . In order to apply this constraint, we need to select events of one interaction for Compton scattering and one interaction for photoabsorption. From theory of error analysis and energy constraint $E_\gamma = E_1 + E_2$, the angular resolution is shown as

$$\Delta\theta = \frac{m_e}{(E_\gamma - E_1)^2 \sin\theta} \Delta(E_\gamma - E_1). \quad (2.2)$$

In the case of gamma ray lines, it is expected that a scintillator detector allows us to achieve sufficient angular resolution for measuring distribution of gamma rays at contamination area. In order to apply the energy constraint, the detector must consist of two layers. Moreover in order to get better angular resolution, we need scintillators which have good energy resolution, such as CsI (Tl), NaI (Tl), and LaBr₃ (Ce). We adopt CsI (Tl) scintillator because it is low-cost (\$50/cm³), slightly hygroscopic and has a dynamic resistance. The size of a CsI (Tl) scintillator cube is 3.5 cm on a side. The size is determined by attenuation length for Compton scattering. The detection efficiency can be improved by increasing the thickness of the absorber of the second layer. However we normalized in size 3.5 cm from the point of view of the cost. Considering the measurement at contamination area, the angular resolution should be $< 5^\circ$. If so when we measure the distribution of gamma rays with this angular resolution, we can detect a 1 m² hot spot which is located 10 m from a detector. In order to keep this angular resolution, each layer is separated about 40 cm. The size of each layer is 24 cm \times 24 cm to provide a 60° wide field of view.

2.3 Prototype detector

Based on the above concept, we developed a prototype detector. Fig. 2 shows a schematic of our Compton camera. Each layer consists of 8 scintillation detectors (see section 2.3.1). Also, optical cameras are equipped at the center of front panel and back panel. Moreover, a preamplifier board (see section 2.3.2) and an ADC board (see section 2.3.3) are put at the bottom of the detector unit.

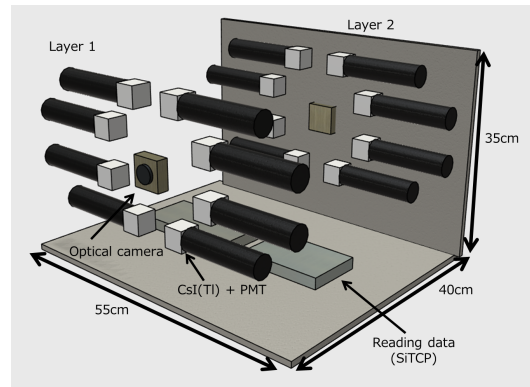


Figure 2: Design of γ I

2.3.1 Scintillation detector

A scintillation detector consists of a CsI (Tl) scintillator cube and a photomultiplier tube (PMT). The PMT (H11432-100) manufactured by Hamamatsu Photonics is a current-output type photomultiplier tube assembly that contains a 38 mm diameter head-on PMT and a Cockcroft-Walton high voltage power supply.

2.3.2 16 channel preamplifier board

We use a non-inverting amplifier which has charge integrating circuit. As an operational preamplifier, we use AD8009 which is developed by Analog Devices. The AD8009 is ultra low noise ($1.9 \text{ nV}/\sqrt{\text{Hz}}$). Signals from PMTs are amplified and shaped by a preamplifier. We use a preamplifier board which has 16 amplifiers on the board.

2.3.3 ADC board

We adopted a 16 channels ADC board with SiTCP technology [5] which was developed by KEK in Japan. The SiTCP is a hardware-based TCP/IP processor. The processor is small circuit size, high-speed data transfer (1 Gbps) with TCP, and users can optimize the protocol for their applications. This ADC board size is $13 \text{ cm} \times 10 \text{ cm}$, and the weight is light (97 g).

After amplification, signals are fed into the SiTCP board. First, waveforms of these signals are digitized by flash ADC chips. After that, these signals are fed into FPGA. These signals are divided into two groups in the FPGA. One is memorized by a PROM. Another is used to generate a trigger signal. If a signal is over threshold, a $40 \mu\text{s}$ gate signal is generated. In our system, when these signals are detected in FPGA simultaneously from any channel of the first layer and any channel

of the second layer, a trigger signal is output. Then the memorized data is readout, and transferred to a computer via ethernet.

2.4 Calibration

The energy calibration can be done by measuring the energy spectrum of some radiation sources with emissions of known energies. First, in order to decide the threshold to cut electronic noise, we measure the voltage value of electric noise. In this measurement of the voltage, generating the trigger signal is forced. The measured voltage is converted to ADC channel, and its distribution is a Gaussian function. The standard deviation is determined by fitting with gauss function and we set 15σ as threshold. From measurement tests, the standard deviation of our detector is around 2 keV.

Second, we measure the energy spectrum of gamma-ray lines emitted from radio active nuclides in order to determine a relationship between event energy and ADC channel. We subtract the electronic noise from the energy spectrum measured above. After that, we decide a ADC channel corresponding to each energy by fitting with three Gaussian functions (605 keV, 796 keV for ^{134}Cs , and 662 keV for ^{137}Cs).

2.5 Online program

We used Visual C++ 2010 to develop an online program. Also, we adopted ROOT as data analysis framework. The data is fed into a computer, and events are selected by online program for reconstruction. We calculate time lag between data of the first layer and the second layer, and obtain the distribution of time lag. We select the data within time lag $\Delta = \pm 1 \mu\text{s}$ because decay time of CsI (TI) is $1 \mu\text{s}$. After that, we select events with $E_1 < 160 \text{ keV}$ in order to reduce back-scattering events. Fig. 3 shows the distribution of the sum of E_1 and E_2 after selection of data by time lag. Then we select the data energy region within $662 \text{ keV} \pm 40 \text{ keV}$ as shown in Fig. 3. Only these events within this region are used for reconstruction of an image.

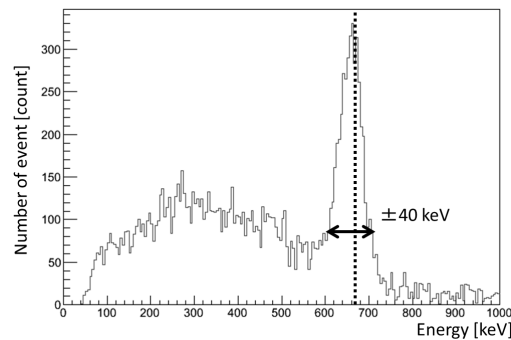


Figure 3: The energy spectrum of ^{137}Cs . We select the events within $662 \text{ keV} \pm 40 \text{ keV}$.

2.6 Laboratory experiment

We measured the distribution of gamma rays from a radiation source in the laboratory. In this measurement test, we used a 1 MBq radiation source of ^{137}Cs , and it was placed 1 m ahead of

the detector. Fig. 4 shows an image taken with the prototype detector. Also, we investigated the angular dependence of acceptance. The angular dependence of acceptance is within $\pm 15\%$ of the average over 60° field of view. The specification of γI is shown in Table 2.6.

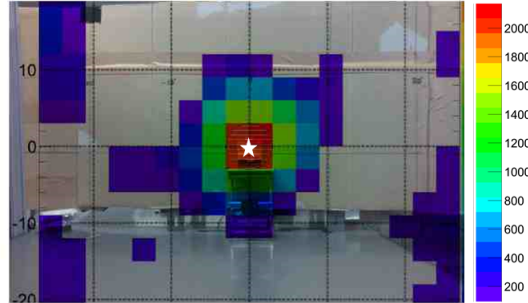


Figure 4: The distribution of gamma rays from ^{137}Cs radiation source. The exposure time was 60 minutes. The source was located 1 m from the detector. The maximum intensity region is shown in red, the level just above average is shown in blue, and the level below the average is shown in transparent. An image reconstructed is superimposed on an image taken with the optical camera at the front panel. The distribution of gamma rays is consistent with the optical image. The symbol of star shows the position of radiation source in the optical picture.

Table 1: The specification of γI

Number of Counters	16
Size of Detector	560 mm \times 400 mm \times 350 mm
Wight of Detector	15 kg
Field of View	$\pm 30^\circ$
Energy Resolution	$\sigma = 25$ keV (at 662 keV)
Angular Resolution	3.5° (using an image sharpening technique)
Detection efficiency	6 cps / (1 $\mu\text{Sv/h}$)

In the case of investigating small hot spots, we can apply an image sharpening technique, which is called "filtered back projection" [7]. We apply a high-pass filter to the original probability distribution function. By accumulating events which are reconstructed by the new function, an image gets sharper. The result obtained by applying this technique will be shown in Section 3.

3. Results

We performed a measurement test in Fukushima city. In this measurement, we set the detector on a lift at a hight 4 m in order to cover a wide area. In the field tests, we extracted events with energies of 605 keV, 662 keV, 796 keV from ^{137}Cs and ^{134}Cs . Fig 5 shows the result of the measurement distribution of gamma rays. One of the hot spots was at the bottom of the trees. Another spot was an area between the trees and the road made of concrete. The distribution of gamma rays detected with γI was consistent with the result of measurements by using a survey meter.

After that, we measured the distribution of the same hot spot from another angle. We confirmed that the same spot can be detected again as shown Fig. 6.

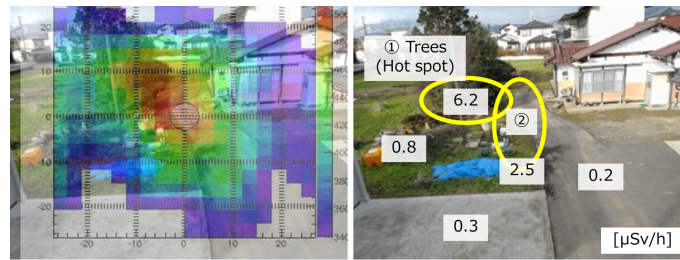


Figure 5: This figure shows the result of the measurement of gamma-rays distribution with γI . The exposure time was 90 minutes, and the distance was 15 m from the detector. The maximum intensity region was a hot spot which is shown in red (left). The right figure shows the dose rate measured by using a survey meter. The dose rate of hot spot was $6.2 \mu\text{Sv/h}$ at the bottom of the trees.

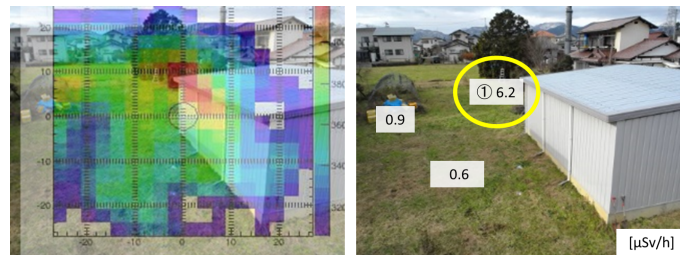


Figure 6: This shows the result of measurement the same hot spot from another angle. The exposure time was 60 minutes, and the distance was 12 m from the detector. The hot spot at bottom of trees was detected again.

Also we measured the distribution of gamma rays beside a garage in Fig. 7. There was a small hot spot. Thus we applied the image sharpening technique to an image of small hot spot. Fig. 7 shows the effect of the image sharpening technique. By applying this technique, the image got sharper.

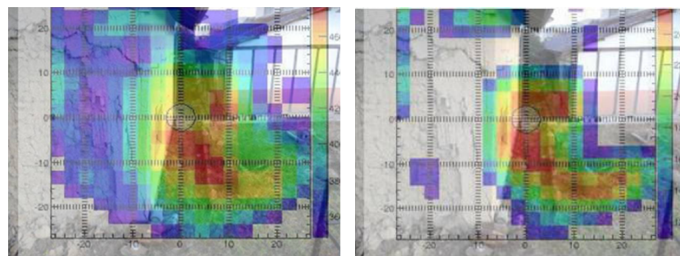


Figure 7: This figure shows the effect of an image sharpening technique. In this measurement, the exposure time was 60 minutes. By using the technique, an image got sharper (right).

4. Discussion and conclusion

We developed a Compton camera γI for measuring distribution of gamma rays in Fukushima. Our detector uses CsI (TI) scintillators in order to achieve high detection efficiency and low-cost. This detector has two layers. Each layer has 8 scintillation detectors which consist of CsI (TI) scintillator cubes, 3.5 cm on a side and super bialkali PMTs. From the result of the laboratory

experiments, the detection efficiency is calculated to be 6 cps / ($\mu\text{Sv/h}$). The field of view is $\pm 30^\circ$. The angular dependence of acceptance is within $\pm 15\%$ of the average over 60° field of view. This detection efficiency is typically more than 10 times better than other detectors for the same purpose. Also, angular resolution is 3.5° by using an image sharpening technique. Moreover the cost is below \$100,000. Then we did the field tests at Fukushima city. We demonstrated the capability of our detector for measurement of arrival direction of gamma rays in the environment even with the dose rate around $1 \mu\text{Sv/h}$. We also demonstrated that an image sharpening technique is effective for detection of small hot spots.

In future, the mass production will be done soon. Also, we have some future plans. One is development of a detector for measuring contamination distribution at a nuclear medical facility. Prototype detectors are already being developed, and these detectors are 360° panorama monitoring detectors. By applying these techniques, we will also design a detector for measurement of gamma ray lines for astrophysics.

References

- [1] K. Okada, T. Tadokoro, Y. Ueno, J. Nukaga, T. Ishitsu, I. Takahashi, Y. Fujishima, K. Hayashi and K. Nagashima *Development of a gamma camera to image radiation fields*, Progress in Nuclear Technology, vol. 4 (2014), pp. 14-17
- [2] T. Kamae, R. Enomoto, and N. Hanada., *A new method to measure energy, direction and polarization of gamma-rays*, Nuclear Instrument & Method in Physics Research A vol. 260 (1987), pp. 254-257
- [3] T. Takahashi, S. Takeda, H. Tajima, S. Watanabe *Visualization of Radioactive Substances with a Si/CdTe Compton Camera*, in proceedings of IEEE Nuclear Science Symposium, (2012)
- [4] J. Kataoka, A. Kishimoto, T. Fujita, K. Takeuchi, T. Kato, T. Nakmaori, S. Ohsuka, S. Nakamura, M. Hirayanagi, S. Adachi, T. Uchiyama, K. Yamamoto, *Handy Compton camera using 3D position-sensitive scintillators coupled with large-area monolithic MPPC arrays*, Nuclear Instruments & Methods in Physics Research A, vol. 732, pp. 403-407
- [5] T. Uchida, *Hardware-Based TCP Processor for Gigabit Etehrnet*, IEEE Transactions on Nuclear Science, vol. 55, no. 3 (2008), pp. 1631-1637
- [6] Rene Brun and Fons Rademakers, *ROOT - An Object Oriented Data Analysis Framework*, Proceedings AIHENP'96 Workshop, Lausanne, Nuclear Instrument & Method in Physics Research A, vol. 389 (1997), pp. 81-86
- [7] Lucas Parra, *Reconstruction of cone-beam projections from Compton scattered data*, IEEE Transactions on Nuclear Science. vol. 47, no. 4, part II (2000), pp. 1543-1550